Interfacial structure and half-metallic ferromagnetism in Co₂MnSi-based magnetic tunnel junctions

N. D. Telling,[1] P. S. Keatley,[2] G. van der Laan,[1] R. J. Hicken,[2] E. Arenholz,[3] Y. Sakuraba,[4] M. Oogane,[4]
Y. Ando,[4] and T. Miyazaki[4]

[1]*Magnetic Spectroscopy Group, CCLRC Daresbury Laboratory, Warrington WA4 4AD, United Kingdom*
[2]*School of Physics, University of Exeter, Stocker Road, Exeter EX4 4QL, United Kingdom*
[3]*Advanced Light Source, Lawrence Berkeley National Laboratory, Berkeley, California 94720, USA*
[4]*Department of Applied Physics, Graduate School of Engineering, Tohoku University, Aoba-yama 6-6-05, Sendai 980-8579, Japan*

X-ray absorption (XAS) and x-ray magnetic circular dichroism (XMCD) techniques are utilized to explore the ferromagnetic/barrier interface in Co₂MnSi full Heusler alloy magnetic tunnel junctions. Structural and magnetic properties of the interface region are studied as a function of the degree of site disorder in the alloy and for different degrees of barrier oxidation. Photoelectron scattering features that depend upon the degree of L2₁ ordering are observed in the XAS spectra. Additionally, the moments per 3d hole for Co and Mn atoms are found to be a sensitive function of both the degree of L2₁ ordering and the barrier oxidation state. Significantly, a multiplet structure is observed in the XMCD spectra that indicates a degree of localization of the moments and may result from the half-metallic ferromagnetism (HMF) in the alloy. The magnitude of this multiplet structure appears to vary with preparation conditions and could be utilized to ascertain the role of the constituent atoms in producing the HMF, and to examine methods for preserving the half-metallic state after barrier preparation. The changes in the magnetic structure caused by barrier oxidation could be reversed by inserting a thin Mg interface layer in order to suppress the oxidation of Mn in the Co₂MnSi layer.

I. INTRODUCTION

Materials possessing the unusual property of half-metallic ferromagnetism (HMF) have recently become of great interest for "spintronics" applications, such as magnetic random access memory (MRAM).[1–3] In these materials the band structure for the two different spin states (majority and minority) is very different. While the majority spin states have metallic character with a nonzero density of states (DOS) at the Fermi level, the minority spin states show a semiconducting character with a band gap. Since spin transport processes depend on the DOS at the Fermi level, materials possessing HMF have the potential to exclude all minority spin electrons and are thus said to have 100% spin polarization. To date there are many materials predicted to show HMF at room temperature (RT) and of these, the L2₁ ordered full Heusler alloy Co₂MnSi (CMS) is a strong candidate for spintronic applications due to its high Curie temperature (985 K). However, for spin-transport processes it is the interface rather than bulk properties that are of importance, as demonstrated by the interface sensitivity of the tunneling magnetoresistance (TMR) effect.[4] The TMR ratio is the percentage change in resistance upon applying a magnetic field and is measured by fabricating a structure called a magnetic tunnel junction (MTJ).[5,6] The resistance is obtained by measuring the tunneling current across a barrier layer (typically alumina or MgO) in the MTJ as the magnetic field is varied.

Currently, the largest TMR for an alumina-barrier-based structure was recorded for a CMS/alumina tunnel junction[7] with a value as high as 570% at low temperature and ∼70% at room temperature. However, TMR probes the *effective* spin polarization at the interface since it is sensitive to spin-flip scattering and the effect of structural and magnetic irregularities both at the interfaces and within the barrier layer. It is thus difficult to isolate the influence of various sample parameters on the HMF at the interface. Such a step is extremely important if the origin of HMF is to be fully understood and thus, the spin-polarization in these materials maximized.

X-ray absorption spectroscopy (XAS) and x-ray magnetic circular dichroism (XMCD) have proved to be effective techniques to probe the electronic and magnetic structure at interfaces. To date there have been several studies that utilized these techniques to examine the interfacial properties of materials used in magnetic tunnel junctions.[8–16] Some of this work has focused on the Heusler-alloy-based MTJs, where the electronic and magnetic structure at the interfaces has been investigated for different sample preparations.[12–16] However, so far the roles of interface ordering and barrier oxidation on the HMF have not been systematically investigated.

In this paper we separately examine the effects of interface ordering and oxidation on the XAS and XMCD spectra in CMS-based structures. We identify features in the XAS caused by photoelectron scattering that can be correlated with the degree of L2₁ site disorder in the CMS layer. We also determine the element-specific magnetic moments per 3d hole as a function of both interfacial ordering and oxidation. Most significantly, however, we observe a multiplet structure in the XMCD spectra that suggests the formation of localized moments on both Mn and Co interface atoms and might be regarded as the signature of HMF in the CMS layer. It is found that this multiplet structure is sensitive to both the degree of site disorder and the oxidation of Mn at the interface following barrier formation. We further show that all the changes ascribed to the effect of Mn oxidation can be re-

TABLE I. Preparation parameters for the sample series studied. In addition to the layer sequencing, annealing temperatures and barrier oxidation times are given. All samples were prepared on MgO(100) single crystal substrates covered with a Cr(100) 40 nm buffer layer.

Sample/series index	Structure MgO(100)/Cr(100)[40_nm]/+...
A_x	Co$_2$MnSi(100) [30 nm+anneal at x °C]/Al[1.3 nm] where x=RT, 300, 400, 450, 500
B_y	Co$_2$MnSi(100) [30 nm+anneal at 450 °C]/Al[1.3 nm +plasma oxidation for y seconds] where y=0, 10, 50, 240
B'	Co$_2$MnSi(100) [30 nm+anneal at 450 °C]/Al[1.3 nm +plasma oxidation for 50 s +2nd anneal at 250 °C]
C	Co$_2$MnSi(100) [30 nm+anneal at 450 °C]/Mg[1 nm]/ Al[1 nm+plasma oxidation for 50 s]

versed by the insertion of a thin Mg layer that prevents oxygen diffusion from the alumina into the CMS layer.

II. EXPERIMENTAL

Epitaxial (100)-oriented CMS layers were prepared on Cr-buffered MgO(100) substrates at ambient temperature using inductively coupled plasma (ICP) assisted magnetron sputtering. A composition-adjusted sputtering target (43.7% Co, 27.95% Mn, 28.35% Si) was used to achieve stoichiometric CMS film composition. Four different sample types were prepared by this method, as summarized in Table I. In the first series (A) the CMS layer was subsequently *in-situ* annealed at different temperatures in order to vary the degree of L2$_1$ site disorder. Following annealing, a 1.3-nm Al capping layer was deposited to prevent oxidation of the CMS layer. In the second series (B) the CMS layer was annealed at 450 °C before depositing the 1.3-nm Al layer. The structure was then plasma oxidized for varying durations to form an alumina barrier layer. One sample (B′) was annealed additionally in a high-vacuum system at a temperature of 250 °C, in the presence of an applied magnetic field of 300 Oe. A further sample (C) was formed from a multilayer stack with an additional 1-nm Mg layer inserted between the CMS layer and alumina barrier. The transport measurements were performed on the equivalent tunnel junction samples made in separate growth runs using a standard four-point probe technique at temperatures between 2 K and RT.

XAS and XMCD measurements were performed at the Advanced Light Source on beamline 6.3.1, providing 65% circularly polarized soft x rays. The x-ray absorption spectra were collected using the total electron yield (TEY) method of detection with the sample inclined at an angle of 30° to the x-ray beam. XMCD was collected at fixed photon helic-
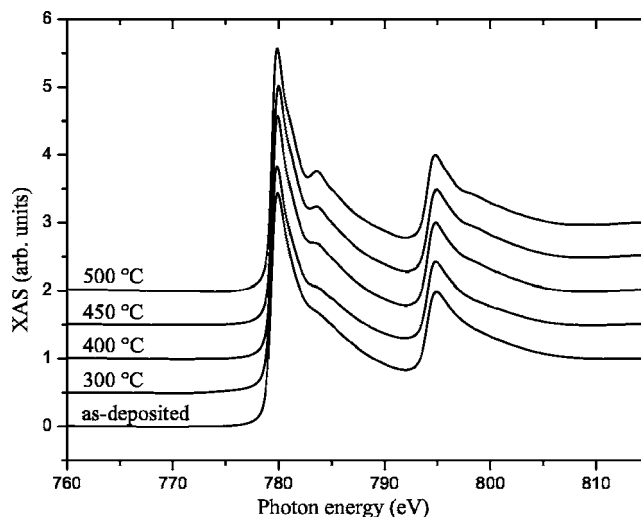

FIG. 1. XAS spectra measured at the Co $L_{2,3}$ absorption edges as a function of annealing temperature of the Co$_2$MnSi layer (series A). The curves have been offset vertically for clarity.

ity by reversing the magnetic field of 500 Oe along the x-ray beam for each photon energy point in the scan.

III. RESULTS AND DISCUSSION

A. Interfacial site disorder

Bulk x-ray diffraction (XRD) measurements (not shown) performed on samples from series A indicated that the degree of L2$_1$ site disorder reduces as a function of annealing temperature but is optimal at 450 °C.[17] The XAS curves measured at the Co $L_{2,3}$ absorption edges for a series of annealing temperatures (series A) are shown in Fig. 1. The most significant features are the pronounced shoulders appearing after the $L_{2,3}$ main lines. The intensity of these shoulders increases dramatically with annealing temperature and thus correlates with the degree of L2$_1$ ordering determined by XRD. These features were seen before in the Co $L_{2,3}$ absorption spectra from L2$_1$ ordered Heusler films,[13,15,16] although their origin remained so far unexplained.

Similar, although substantially weaker, shoulders were observed in the Mn $L_{2,3}$ spectra. Figure 2 shows the XAS measured at the Mn $L_{2,3}$ edges for the as-deposited (least well ordered) and optimum annealed (most ordered) CMS films. The corresponding Co absorption spectra are reproduced for comparison. By aligning the XAS spectra at a common zero energy (corresponding to the half-height point of the L_3 peak) it can be seen that the shoulders appearing just after the L_3 edge are at the same energy position for Co and Mn. A simple estimate of the photoelectron wavelength for this feature using $\lambda \approx 12.3/[E(eV)]^{1/2}$, where E is the photoelectron energy, gives a value of ~5.9 Å. This is close to the lattice parameter of the ordered L2$_1$ alloy (a =5.65 Å), which suggests that the origin of the shoulder could be photoelectron scattering from the ordered superlattice. This scattering structure is due to the interference of emitted photoelectrons by the potential of the neighboring atoms and is thus sensitive to the local environment. Peaks in
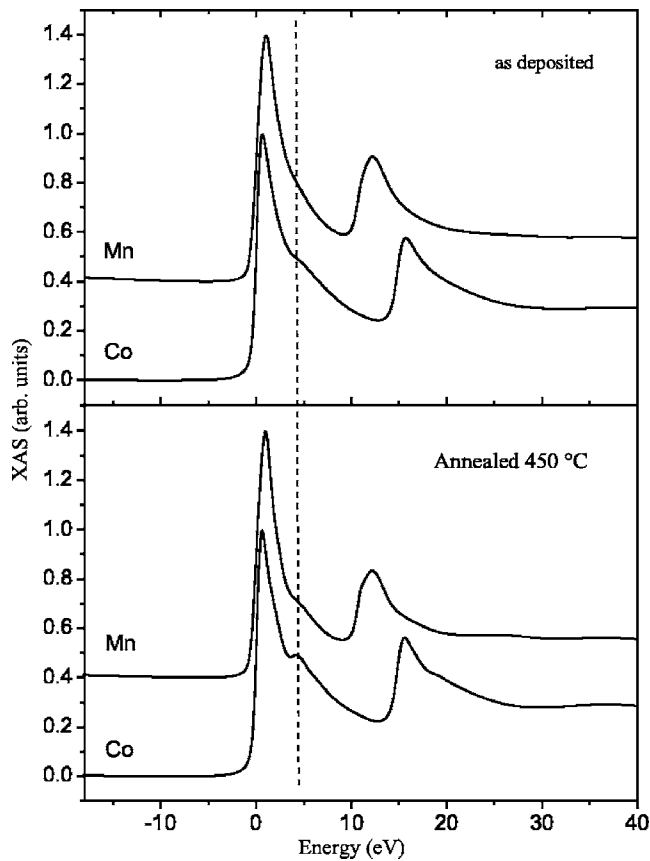
FIG. 2. XAS spectra measured at the Co and Mn $L_{2,3}$ absorption edges for Co_2MnSi layers in the as-deposited state (sample A_{RT}) and for optimum annealing temperature (A_{450}). The zero energy origin corresponds to half the L_3 peak height for each curve. The curves have been scaled to unity at the L_3 peak maximum and offset vertically for clarity. The dashed line shows the common position of the shoulder feature in both Co and Mn spectra.

the soft x-ray absorption near edge structure (XANES) region have been observed previously for Co films[18] but are generally much weaker than the features seen here. The reason for this clearly pronounced shoulder could be the large lattice parameter of the ordered superlattice that leads to XANES features within the strong absorption region of the L_3 white line.

In addition to the shoulder features in the XAS, extended x-ray absorption fine structure (EXAFS) oscillations were also observed, as shown in Fig. 3. The amplitude of these fringes also increases with annealing temperature (and thus, L2$_1$ site ordering). As there is no contribution from the electronic structure in this region, this observation proves that the photoelectron scattering is enhanced with increasing L2$_1$ ordering. This confirms our conclusion that photoelectron scattering from the L2$_1$ structure is also responsible for the shoulder just after the L_3 peak in the absorption spectrum, i.e., that this is a (XANES) feature related to the crystalline structure of the ordered superlattice and does not arise from the electronic structure.

XMCD measurements were performed on sample series A to ascertain the effect of annealing temperature on the element-specific magnetic moments. As the precise $3d$ hole
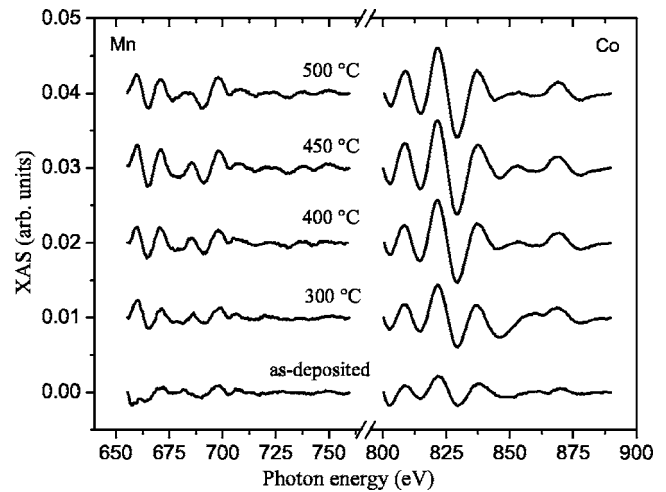

FIG. 3. EXAFS oscillations measured after the L_2 absorption edges for Mn and Co as a function of annealing temperature (series A). The XAS background has been removed by spline curve fitting and the curves have been offset vertically for clarity.

count for Co and Mn atoms in CMS is not known, we determined instead the total moments per $3d$ hole by applying sum rule analysis following a standard procedure detailed elsewhere.[19] The results of this analysis are plotted in Fig. 4 and show a doubling of the moments of both Co and Mn atoms after annealing. This result is consistent with bulk magnetization measurements on similar samples.[17] We note, however, that in contrast to previous XMCD results reported on CMS,[16] we record here a substantial moment on both Co and Mn atoms even in the as-deposited CMS film. This result probably reflects the high quality of the epitaxial films in the as-deposited sample discussed here as compared to the earlier polycrystalline films.

B. Barrier oxidation

We discuss now the impact on the interfacial properties of an optimally ordered CMS film (450 °C anneal) following plasma oxidation of the Al layer to form an alumina barrier. No significant differences were observed between samples from series B and the sample with a second anneal following barrier preparation (B′). Thus we will discuss only samples from series B. The total moments per $3d$ hole determined as a function of barrier oxidation time for these samples (series B) are also shown in Fig. 4. It is evident that the Co moment is enhanced by ~15% after plasma oxidation for 50 s, while the Mn moment is reduced by roughly the same percentage. The 50-s oxidation time was found to be optimal for the TMR of the equivalent MTJs, with values of ~70% at RT and ~150% at 2 K being recorded.[20]

The enhancement in Co moment for the optimum oxidation time is consistent with our previous measurements on Co/alumina-based MTJs[11] and might be related to a change in interfacial bonding following barrier oxidation. The reduction in Mn moment, however, is likely to be caused by the formation of paramagnetic Mn oxide at the CMS/alumina interface. Evidence of this oxide formation is seen in the XAS spectra shown in Fig. 5(a). The CMS/alumina film
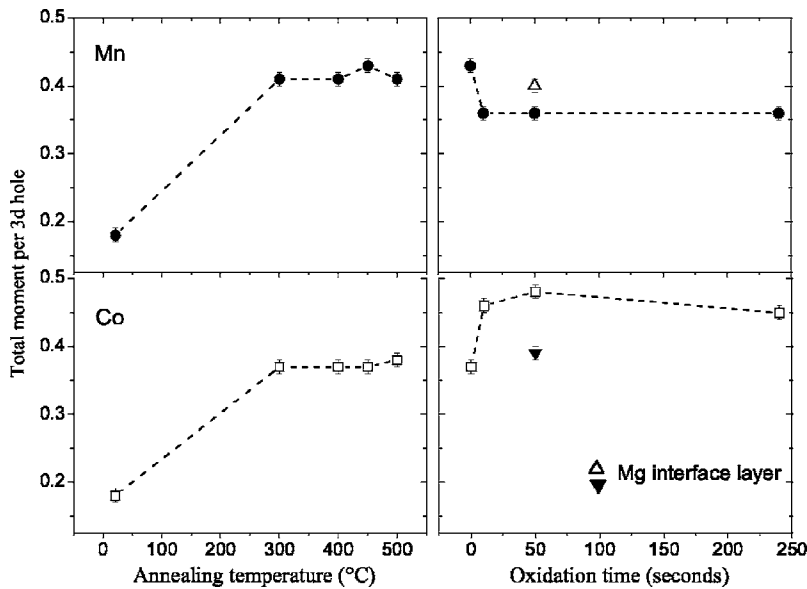
FIG. 4. Total moment per $3d$ hole measured for Mn (top panels) and Co atoms (lower panels). The left-hand plots show the values measured as a function of annealing temperature (series A), and the right-hand plots show values as a function of barrier oxidation time (series B). The moments measured for a sample prepared with an additional Mg interface layer prior to barrier oxidation (sample C) are also shown.

(B$_{50}$) shows a multiplet structure that is characteristic of Mn ions with a $3d^5$ electronic configuration, such as found for MnO$_x$. The multiplet structure is due to intra-atomic $2p$-$3d$ Coulomb and exchange interaction, spin-orbit interaction, and $3d$ crystal field interaction.[21] In localized systems, such as MnO$_x$, it gives a fingerprint that is characteristic for the configuration of the $3d$ states. It is interesting to see from Fig. 5(a) that the positions of this multiplet structure are not the same as the features attributed earlier to XANES structure in the Mn spectra (i.e., due to photoelectron scattering). Thus we can rule out the possibility of the latter features arising from oxidized Mn.

The corresponding XAS spectra measured at the Co $L_{2,3}$ edges are shown in Fig. 5(b). In contrast to the Mn spectra, the Co spectra show no significant change after barrier oxidation. Thus, any interface oxidation that occurs is localized at the Mn atoms (which have a larger affinity for oxygen

than Co atoms). To further investigate the effect of interface oxidation, a sample (C) was prepared with a thin (1 nm) Mg layer inserted between the CMS and barrier layer to act as a barrier to oxygen diffusion from the alumina. The absence of oxide-related multiplet structure in the Mn XAS curve from this sample [Fig. 5(a)] indicates that the Mg interface layer was successful at preventing Mn oxidation. The corresponding atomic moments per $3d$ hole, determined from XMCD measurements, are given in Fig. 4. It is seen that insertion of the Mg layer almost completely restores both the Co and Mn moments to their original values prior to barrier oxidation. This confirms our findings regarding the opposed variation in Co and Mn moments as a function of barrier preparation and clearly demonstrates the sensitivity of the interface moments to oxidation. The implications of this Mg interface layer on the TMR characteristics of this sample will be discussed in detail elsewhere.[22]
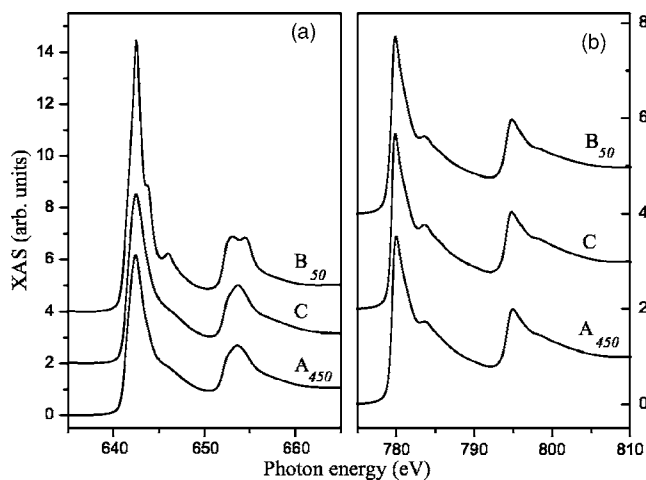
C. XMCD and half-metallic ferromagnetism

The XMCD spectra obtained at the Mn $L_{2,3}$ edges as a function of annealing temperature are shown in Fig. 6. Multiplet structure is observed in the XMCD spectra despite the metallic-like XAS spectra. This structure in the XMCD is indicative of the presence of localized moments such as those observed in magnetic oxides.[23] However, the fact that the multiplet structure is only weakly observed in the corresponding XAS spectra could be related to the half-metallic nature of the ferromagnetism in these films. In a material possessing HMF the moments are in fact localized despite the delocalized character of one of the spin bands.[24] As the XAS probes both majority and minority spin valence states, it might be expected that any multiplet structure observed would be weak since it arises from only one spin band. In contrast, XMCD probes only the polarization of the spin bands and can thus provide evidence of these localized moments from delocalized electrons and serve as a fingerprint for HMF. The inset to Fig. 6 shows a slight variation in the XMCD multiplet structure as a function of annealing tem-
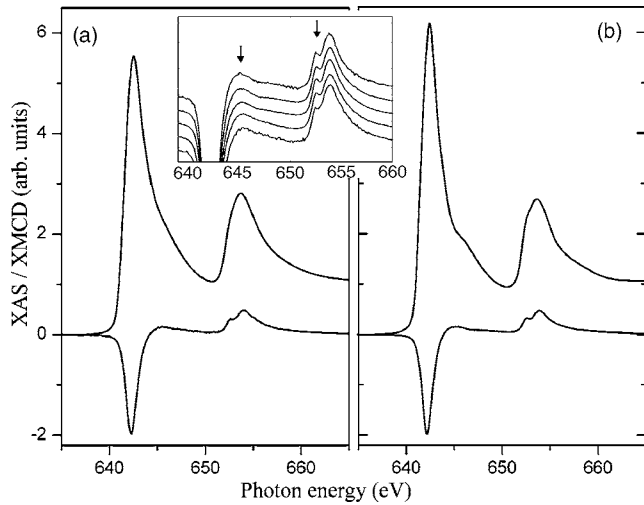

FIG. 5. XAS spectra measured at the Mn and Co $L_{2,3}$ absorption edges for samples with optimum annealing temperature (A$_{450}$) and optimum barrier oxidation time (B$_{50}$). The curves measured for a sample prepared with an additional Mg interface layer prior to barrier oxidation (sample C) are also shown.

FIG. 6. XAS and XMCD spectra (lower curves) measured at the Mn $L_{2,3}$ absorption edges for a Co_2MnSi layer in the as-deposited state (sample A_{RT}) (a) and with optimal annealing temperature (A_{450}) (b). The inset shows an enlargement of the XMCD measured for the entire series, with annealing temperature increasing from the bottom as RT, 300, 400, 450, and 500 °C. The positions of multiplet features in the XMCD curves are indicated by the arrows.

perature. This correlates with the expected improvement in HMF as the CMS layer becomes more ordered.

Evidence of localized moments was also observed in the Co $L_{2,3}$ XMCD spectra [Fig. 7(a)]. Comparison with the XMCD obtained from an aluminum-capped Co thin film re-
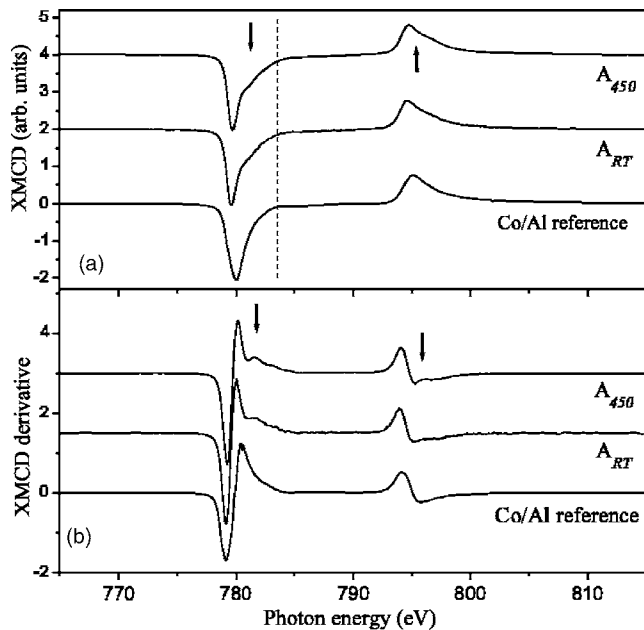

FIG. 7. (a) XMCD spectra measured at the Co $L_{2,3}$ absorption edges for a Co_2MnSi layer in the as-deposited state (A_{RT}) and with optimum annealing temperature (A_{450}). The lower curve is the XMCD measured on a reference sample of a Co thin film capped with Al. Arrows mark the positions of multiplet features. (b) Derivatives of the XMCD spectra shown in (a). All curves have been displaced vertically for clarity.
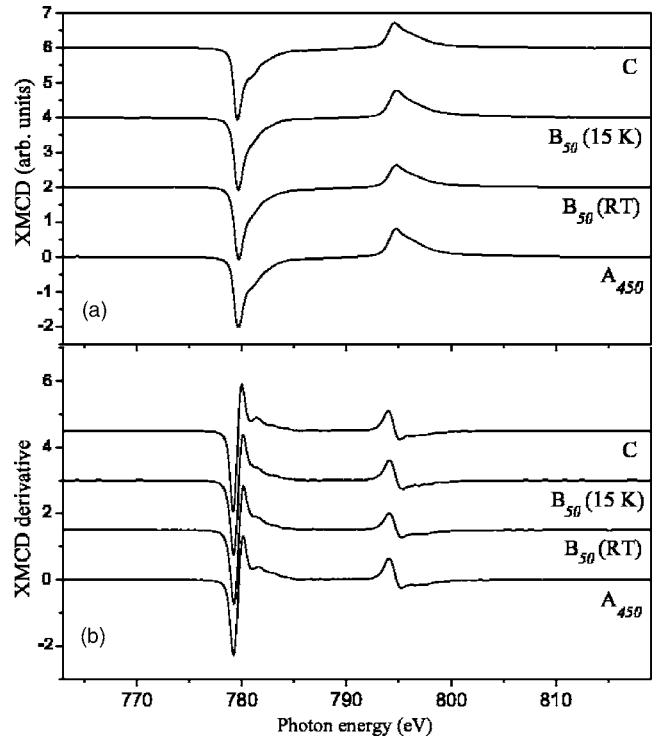

FIG. 8. (a) XMCD spectra measured at the Co $L_{2,3}$ absorption edges for a Co_2MnSi layer with optimal annealing temperature (A_{450}), and following barrier preparation with optimal oxidation time (B_{50}). For sample B_{50}, data is shown for measurements performed at RT and 15 K, while all other spectra shown are for RT measurements. In addition, the XMCD measured on a sample with an interface Mg layer is shown (sample C). (b) Derivatives of the XMCD spectra shown in (a). All curves have been displaced vertically for clarity.

veals the presence of multiplet structure in CMS samples, just after the L_3 and L_2 edges. It should be noted that this multiplet structure does not coincide with the shoulder in the Co XAS spectra [indicated by the dashed line in Fig. 7(a)] and so appears to be unconnected with this feature. As with the Mn XMCD, there is a slight increase in magnitude of the multiplet structure when the film becomes more ordered. These differences are better visible in the derivative curves shown in Fig. 7(b). The presence of localized moments on both Co and Mn atoms in the CMS layers would suggest that both elements are contributing to the HMF. This is in agreement with electronic structure calculations for this system[25] in which the overall band gap is determined from the superposition of the atom-resolved DOS. Crucially, the results presented here indicate that XMCD may be utilized as an element-specific probe of HMF, thus providing important data for model calculations.

The sensitivity of the Co XMCD multiplet features to the interface structure can be seen in Fig. 8. Following oxidation of the aluminum layer to form the barrier, this structure is diminished. Hence it appears that the localized Co moments (and thus HMF) are reduced after barrier preparation. This could be related to the loss of HMF on Mn sites within this MnO_x interface layer, which could then suppress the HMF for Co interface atoms due to the effective removal of Mn

atoms within the $L2_1$ structure. However, it is unlikely that the multiplet structure would completely disappear, as the probing depth for XMCD measured in the TEY detection mode is ~25 Å. There will, therefore, still be a contribution to the XMCD from Co atoms situated beneath the MnO_x region. It was found that the Mn XMCD (not shown) was unaffected by barrier oxidation. This is not surprising since the paramagnetic MnO_x layer formed will not contribute to the XMCD and only the unperturbed region beneath this oxide layer will be probed.

Further evidence of the role of Mn oxidation on localized Co moments can be seen in the sample containing the additional Mg interface layer (Fig. 8). As mentioned above, this Mg layer is effective at suppressing Mn oxidation. If the reduction in multiplet structure (and consequently HMF) is indeed due to Mn oxidation, then it might be expected that this structure would be restored in the Mg-based sample. From inspection of the curves (B_{50} and C) in Fig. 8, it can be seen that this is indeed the case and multiplet features of similar magnitude to the unoxidized sample (A_{450}) are observed. These results thus imply that the HMF at the interface is sensitive to the oxidation state of Mn atoms near the barrier. This has important implications for the preparation of MTJs from this material since the TMR will not only be reduced by spin-flip scattering in the MnO_x layer, but also by the reduction in HMF and hence, spin polarization of the CMS layer at the interface. Avoiding Mn interface oxidation is thus a key challenge for obtaining highly spin-polarized MTJs.

The XMCD shown for the plasma-oxidized sample (B_{50}) is given in Fig. 8 for measurements at both RT and 15 K. Magnetotransport measurements indicate a substantial temperature dependence of the TMR with roughly a twofold increase between RT and 2 K.[26] However, it is seen from Fig. 8 that the magnitude of the multiplet feature is unchanged upon cooling to 15 K. In addition, the Co and Mn moments per 3*d* hole measured between RT and 15 K (to be presented elsewhere[22]) were also found to be temperature independent. Thus, it does not seem that the temperature variation of TMR in these samples is related to a change in the magnetic structure resulting from a magnetic phase transition. Such temperature-dependent effects have, however, been observed in other Heusler systems.[27]

IV. CONCLUSIONS

The ferromagnet/barrier interfaces in CMS/alumina magnetic tunneling structures have been studied using XAS and XMCD in order to examine the effects of site disorder and oxidation. XANES-type features and EXAFS oscillations were observed in the XAS spectra that reflected the degree of $L2_1$ site disorder in the interface region. XMCD measurements were used to determine the element-specific moments per 3*d* hole and further revealed the presence of localized moments despite the delocalized valence state apparent from the XAS spectra. These latter features were attributed to HMF in the CMS layer and suggest that an element-specific measurement of HMF might be possible with these techniques. Such a measurement will be of huge importance for unravelling the role of different atoms on the formation of HMF in the alloy.

It was found that the moments per 3*d* hole together with the degree of localization of the moments (judged by the magnitude of the multiplet structure in the XMCD) were sensitive functions of both the site disorder and interface oxidation. In particular, both the size of the Co and Mn moments and their degree of localization increased with improved $L2_1$ ordering. However, the oxidation of Mn interface atoms during barrier formation led to a reduction in the average Mn moment and was found to partially suppress the localization of Co moments and consequently, the degree of HMF. Significantly, all the effects ascribed to interface oxidation were found to be reversed by inserting a thin Mg interface layer which acted as an oxygen diffusion barrier. This not only demonstrates the validity of these observations, but also suggests mechanisms for preserving the degree of HMF at the CMS/barrier interface. XAS and XMCD can thus provide a powerful tool to complement the magnetotransport-based measurements of spin polarization for this system.

[1] I. Žuitić, J. Fabian, and S. Das Sarma, Rev. Mod. Phys. **76**, 323 (2004).

[2] E. Y. Tsymbal, O. N. Mryasov, and P. R. LeClair, J. Phys. Condens. Matter **15**, R109 (2003).

[3] J. M. D. Coey, M. Venkatesan, and M. A. Bari, Lect. Notes Phys. **595**, 377 (2002).

[4] J. M. de Teresa, A. Barthélémy, A. Fert, J. P. Contour, F. Montaigne, and P. Seneor, Science **286**, 507 (1999).

[5] T. Miyazaki and N. Tezuka, J. Magn. Magn. Mater. **139**, L231 (1995).

[6] J. S. Moodera, L R Kinder, T M Wong, and R Meservey, Phys. Rev. Lett. **74**, 3273 (1995).

[7] Y. Sakuraba, M. Hattori, M. Oogane, Y. Ando, H. Kato, A. Sakuma, T. Miyazaki, and H. Kubota, Appl. Phys. Lett. **88**, 192508 (2006).

[8] J. Schmalhorst, M. Sacher, A. Thomas, H. Brückl, G. Reiss, and K. Starke, J. Appl. Phys. **97**, 123711 (2005).

[9] K. Miyokawa, S. Saito, T. Katayama, T. Satio, T. Kamino, K.

Hanashima, Y. Suzuki, K. Mamiya, T. Koide, and S. Yuasa, Jpn. J. Appl. Phys., Part 2 **44**, L9 (2005).

[10] M. Sicot, S. Andrieu, F. Bertran, and F. Fortuna, Phys. Rev. B **72**, 144414 (2005).

[11] N. D. Telling, G. van der Laan, S. Ladak, and R. J. Hicken, Appl. Phys. Lett. **85**, 3803 (2004); N. D. Telling, G. van der Laan, S. Ladak, R. J. Hicken, and E. Arenholz, J. Appl. Phys. **99**, 08E505 (2006).

[12] J. Grabis, A. Bergmann, A. Nefedov, K. Westerholt, and H. Zabel, Phys. Rev. B **72**, 024437 (2005).

[13] S. Stadler *et al.*, J. Appl. Phys. **97**, 10C302 (2005).

[14] M. Kallmayer, H. J. Elmers, B. Balke, S. Wurmehl, F. Emmerling, G. H. Fecher, and C. Felser, J. Phys. D **39**, 786 (2006).

[15] S. Wurmehl, G. H. Fecher, H. C. Kandpal, V. Ksenofontov, C. Felser, and H.-J. Lin, Appl. Phys. Lett. **88**, 032503 (2006).

[16] J. Schmalhorst, S. Kämmerer, M. Sacher, G. Reiss, A. Hütten, and A. Scholl, Phys. Rev. B **70**, 024426 (2004).

[17] M. Oogane, Y. Sakuraba, J. Nakata, H. Kubota, Y. Ando, A. Sakuma, and T. Miyazaki, J. Phys. D **39**, 834 (2006).

[18] A. I. Nesvizhskii and J. J. Rehr, J. Synchrotron Radiat. **6**, 315 (1999).

[19] C. T. Chen, Y. U. Idzerda, H.-J. Lin, N. V. Smith, G. Meigs, E. Chaban, G. H. Ho, E. Pellegrin, and F. Sette, Phys. Rev. Lett. **75**, 152 (1995); B. T. Thole, P. Carra, F. Sette, and G. van der Laan, *ibid.* **68**, 1943 (1992).

[20] Y. Sakuraba, T. Miyakoshi, M. Oogane, Y. Ando, A. Sakuma, T. Miyazaki, and H. Kubota, Appl. Phys. Lett. **89**, 052508 (2006).

[21] G. van der Laan and B. T. Thole, J. Phys. Condens. Matter **43**, 13401 (1991); G. van der Laan and I. W. Kirkman, Onsei Gengo Igaku **4**, 4189 (1992).

[22] Y. Sakuraba, M. Oogane, Y. Ando, A. Sakuma, T. Miyazaki, and H. Kubota (unpublished).

[23] D. J. Huang *et al.*, J. Electron Spectrosc. Relat. Phenom. **137-140**, 633 (2004).

[24] J. Kübler, A. R. Williams, and C. B. Sommers, Phys. Rev. B **28**, 1745 (1983).

[25] I. Galanakis, K. Özdoğan, B. Aktaş, and E. Şaşioğlu, Appl. Phys. Lett. **89**, 042502 (2006).

[26] Y. Sakuraba, J. Nakata, M. Oogane, H. Kubota, Y. Ando, A. Sakuma, and T. Miyazaki, Jpn. J. Appl. Phys., Part 2 **44**, L1100 (2005).

[27] C. N. Borca, T. Komesu, H.-K. Jeong, P. A. Dowben, D. Ristoiu, Ch. Hordequin, J. P. Nozières, J. Pierre, S. Stadler, and Y. U. Idzerda, Phys. Rev. B **64**, 052409 (2001).